https://doi.org/10.5194/egusphere-2026-6663
Preprint. Discussion started: 16 November 2026
© Author(s) 2026. CC BY 4.0 License.

NOAA Global Systems Laboratory experimental pollen forecasting using the Pollen Emissions for Climate Models (PECM) with the Rapid-Refresh coupled to Chemistry (RAP-Chem) model

Jordan Schnell[1,2], Allison Steiner[3], Ravan Ahmadov[2], Yingxiao Zhang[4], Tamanna Subba[5], Alton Campbell[6], Nathan T. Allan[6], Sagun Kayastha[6], Dustin Fowler[7], Guy Robinson[8,9]
[1]Cooperative Institute for Research in Environmental Sciences (CIRES), University of Colorado, Boulder, Boulder, CO 80309, USA
[2]NOAA Global Systems Laboratory, 325 Broadway, Boulder, CO 80305, USA
[3]University of Michigan, Ann Arbor, MI 48109, USA
[4]NSF National Center for Atmospheric Research (NCAR), Boulder, CO 80301, USA
[5]Brookhaven National Laboratory, P.O. Box 5000, Upton, New York 11973, USA
[6]Pollen Sense, LLC, Provo, UT 84604, USA
[7]Allergy and Asthma Care of Waco, 221 Jewell Drive Waco, TX 76712
[8]Department of Natural Sciences, Fordham University, New York, NY 10023
[9]Louis Calder Center, Armonk, NY 10504

Correspondence to: Jordan Schnell (*jordan.schnell@colorado.edu*)

Abstract. Pollen impacts millions of Americans, yet US-based operational models lack its representation. We evaluate real-time, tree, grass, and weed pollen forecasts from the Rapid-Refresh coupled to Chemistry (RAP-Chem) model and the Pollen Emissions for Climate Models version 2 (PECM v2.0) across North America for 2025. We evaluate RAP-Chem using counts from National Allergy Bureau (NAB) stations and a novel observational product from Pollen Sense. Pollen Sense correlated moderately with NAB (Spearman r = 0.50–0.70) and demonstrated moderate skill in reproducing phenology (start, peak, and end-of-season; SOS/POS/EOS), with mean absolute errors (MAE) for tree, grass, and weed pollen of 21.0/13.9/22.4 d; 5.2/18.4/6.6 d, and 19.2/44.2/21.4 d, respectively validating its spatial evaluation utility. At NAB stations, RAP-Chem best simulates weed pollen (r(NAB) = 0.74, r(Pollen Sense) = 0.75), followed by grass (0.53, 0.36) and tree (0.40, 0.29) pollen, with similar skill to Pollen Sense in reproducing NAB phenology (MAE = 19.9/20.7/13.8 d, 24.0/17.6/12.2 d, and 32.8/65.2/12.2 d). Total pollen has correlations r(NAB) = 0.44 and r(Pollen Sense) = 0.42. US-wide, RAP-Chem and Pollen Sense phenology agree best for weed pollen. RAP-Chem underestimates tree and grass pollen at most NAB sites and overestimates Pollen Sense tree pollen in forested areas. RAP-Chem grass and weed pollen magnitudes strongly depend on a post-processing correction for model-omitted gravitational settling, while correlation and phenology are unaffected. This experimental framework marks a critical advancement toward pollen forecasting and public health exposure management in the US.

https://doi.org/10.5194/egusphere-2026-6663
Preprint. Discussion started: 16 November 2026
© Author(s) 2026. CC BY 4.0 License.

1 Introduction

Pollen is an airborne bioaerosol emitted from plants as part of their biological reproductive cycle. Around 25% of the US population experiences seasonal allergies, largely due to exposure to airborne pollen (Ng and Boersma, 2023). Symptoms from pollen exposure range from minor allergic rhinitis to severe reactions such as anaphylaxis, which result in billions of dollars in healthcare costs (Meltzer and Bukstein, 2011) and lost work productivity (Crystal-Peters et al., 2000). Despite these widespread impacts, pollen is neither regulated as an air pollutant (https://www.epa.gov/criteria-air-pollutants) nor included in operational National Weather Service (NWS) numerical weather prediction (NWP) or air quality forecasts (https://forecast.weather.gov/product_types.php). Furthermore, unlike criteria pollutants such as particulate matter with diameters less than 2.5 μm and 10 μm ($PM_{2.5}$ and PM_{10}, respectively), the US Environmental Protection Agency (EPA) does not maintain a federally operated or partnered network to measure ambient pollen concentrations.

Consequently, pollen monitoring and forecasting are largely dominated by the private sector. The primary observational network is sponsored by the National Allergy Bureau (NAB) of the American Academy of Allergy, Asthma, and Immunology (AAAAI)(https://pollen.aaaai.org/). While considered the observational "gold standard" (Shah et al., 2024), the NAB's ~100 US sites rely heavily on manual counting, providing separate (where available) tree, grass, and weed (and often mold) counts every 1–3 days. Counts are often unavailable on weekends and holidays and are reported with a one-day delay. The process is extremely labor intensive, which contributes to the lack of government sponsored networks. The recent deployment of automated pollen sensor networks (e.g., Pollen Sense; https://pollensense.com/) offers the potential to greatly expand pollen monitoring across the US and beyond, with 100s of monitors already deployed globally. By design, the automated sensors require minimal human intervention, and as such can provide higher frequency (e.g., hourly), near-real-time pollen counts in locations without dedicated research, medical, or laboratory facilities that are typically located in urban or heavily populated areas.

In the absence of government-led forecasting, commercial applications provide opaque pollen "forecasts." These commercial products are typically empirical, likely combining persisted NAB measurements, climatological seasonal cycles, and basic meteorological relationships (e.g., https://www.pollen.com/help/faq#faq2), rather than dynamically simulating atmospheric transport or the rupture of intact pollen grains into sub-pollen particles (SPPs). Pollen emission models generally fall into two categories: process-based (simulating plant-scale emissions via complex biochemistry and environmental and phenological criteria) and empirical (using observed relationships between pollen counts and meteorology)(Scheifinger et al., 2013). The Pollen Emissions for Climate Models (PECM) is a notable empirical emissions model (Wozniak and Steiner, 2017; Zhang and Steiner, 2022) that has been successfully coupled to a coupled chemistry climate model, namely the Weather Research and Forecasting model with Chemistry (WRF-Chem; Grell et al., 2005)(Subba et al., 2023; Zhang et al., 2024). Using a model like WRF-Chem to simulate pollen emissions, transport, and physics-based loss processes (e.g., wet scavenging, dry deposition, rupture) provides a critical advantage over standard empirical forecasts. Transport and rupture are especially important for determining the health impacts of SPPs, which are much smaller than intact pollen grains and

https://doi.org/10.5194/egusphere-2026-6663
Preprint. Discussion started: 16 November 2026
© Author(s) 2026. CC BY 4.0 License.

can be transported significantly farther than intact grains due to their multiple orders of magnitude smaller size. Additionally, a model like WRF-Chem can be used to quantify the impact of intact pollen and SPPs on meteorological forecasts (see below). Currently, the combination of sparse observational networks and a dearth of coupled emission–transport models has left the distribution of pollen both within and beyond the planetary boundary layer poorly constrained (Subba et al., 2023). Beyond human health, pollen interacts dynamically with the atmosphere. Like other aerosols, pollen scatters incoming solar radiation and alters cloud and precipitation processes by acting as cloud condensation nuclei (CCN; Steiner et al., 2015) and ice nucleating particles (INP; Matthews et al., 2023). Intact pollen, due to its large size and high hygroscopicity, can act as giant CCN (Posselt and Lohmann, 2008; Tang et al., 2019; Yin et al., 2000). Because integrating aerosols into NWP improves overall meteorological forecast accuracy (Coye et al., 2026; James et al., 2022; Zhang et al., 2022), including pollen might offer a dual benefit for health and weather prediction. Recognizing this, the experimental Rapid-Refresh model coupled to Chemistry (RAP-Chem; Schnell et al., 2026) began producing hourly predictions of intact and ruptured pollen using PECM in July 2022 at a resolution of 13.5 km. By spring 2025, this capability was expanded to explicitly delineate intact tree, grass, and weed pollen beyond the prior lumped total intact pollen.

Here we present the first comprehensive evaluation of the real-time RAP-Chem speciated pollen forecasts for a full calendar year (1 January – 31 December 2025). We evaluate the model using a subset of NAB stations alongside a novel gridded observational product derived from the Pollen Sense automated optical sensor network. Sect. 2 describes the observational datasets, the RAP-Chem model, and the evaluation methods. Sect. 3 compares the NAB sites and Pollen Sense product and presents the evaluation of RAP-Chem against both NAB and Pollen Sense. Finally, Sect. 4 summarizes our findings and discusses future directions for pollen forecasting.

2 Data and methods

2.1 Observations and model comparison products

2.1.1 AAAAI/NAB pollen counts

We utilize daily pollen counts from nine sites in the AAAAI NAB network (Table S1). The nine sites were chosen due to their open access to historical counts, which are provided on public facing websites. The NAB sites use a volumetric sampling (i.e., the Hirst-type or Rotorod) method and trained pollen identification experts to count individual plant taxa. Not all sites count and/or do not display on their website the same pollen families and/or genera, with some only providing a total pollen count. The sites used herein are primarily located in the eastern and central US, except for the station in Boise, ID. Three sets of pollen stations are located in relatively close proximity to one another (i.e., St. Louis, MO and Springfield, MO; Armonk, NY and New York, NY; and Waco, TX and Houston, TX), somewhat limiting the geographical diversity in the dataset as a whole, but at the same time offering perspective into local-to-regional pollen dynamics. Other sites offer perspectives into unique pollen emission behavior. For example, the Waco, TX station sits in multiple climate zones and has

https://doi.org/10.5194/egusphere-2026-6663
Preprint. Discussion started: 16 November 2026
© Author(s) 2026. CC BY 4.0 License.

a distinct winter tree pollen (mountain cedar in the Cupressaceae family), which is somewhat unique to the rest of the country.

2.1.2 Pollen Sense

We additionally utilize a dataset obtained from the Pollen Sense network of sensors (https://PollenSense.com/). Traditional volumetric methods employed by the NAB stations require a trained analyst to manually count and classify collected pollen grains. Pollen Sense's automated, portable sensors (APS-400), however, draw ambient air across an optical path and capture high-resolution images of individual airborne particles (with diameters ranging from approximately 3–120 μm) that are classified by a convolutional neural network trained on a continuously expanding library of over 10^6 images, allowing near-real-time identification without human intervention. Although Pollen Sense can resolve individual pollen genera (e.g., *Ambrosia*), under our data sharing agreement, we receive counts aggregated into three broad classes (tree, grass, and weed pollen). RAP-Chem's tree, grass, and weed tracers are compared against the same aggregated observations (see Sect. 2.2 and 2.3). Thus, genus-level discrepancies within a class (e.g., over-predicting *Quercus* while under-predicting *Betula*) are not resolvable and may partially cancel one another. Because the different genera have differing grain sizes, phenology, and emission behaviors, weed pollen, which over our domain is dominated by a single genus (*Ambrosia*), is expected to exhibit the strongest agreement. The Pollen Sense (and PECM-RAP-Chem, Sect. 2.2) tree class aggregates the widest diversity of taxa and grain sizes (Table S2).

Prior to distribution outside of Pollen Sense, counts from individual sensors are spatially interpolated onto a 30 km × 30 km grid. For each sensor and grid cell, an 11-year (2015–2025) baseline land surface temperature from the Moderate Resolution Imaging Spectroradiometer (MODIS) Terra satellite (https://doi.org/10.5067/MEaSUREs/LSTE/CAM5K30UC.003) and surface insolation from CERES FlashFlux (https://doi.org/10.5067/TERRA-AQUA/CERES/FLASH_TISA_L3.004A) is extracted and averaged across the weeks centered on the spring equinox. Each grid cell is assigned the inverse-distance-weighted mean of its four nearest sensors, where distance is the horizontal separation plus scaled differences in climatological temperature and irradiance between the sensor and the cell. Hourly fields are then averaged to daily values. The interpolation preserves the anonymity of private sensor owners and keeps the shared product within the free data service tier. The gridded product (30 km) inherently smooths fine-scale spatial gradients and is also a coarser resolution compared to RAP-Chem (13.5 km; Sect. 2.3). Thus, many grid cells reflect interpolation rather than measurement and should be interpreted with caution. During the periods analyzed, the network comprised approximately 90–105 sensors covering much of the contiguous United States, albeit with several notable gaps (Fig. S1). Sensors are concentrated near metropolitan areas and are frequently colocated with existing NAB stations (Sect. 2.1.1), providing a valuable cross-validation between the two networks. Sensor density is greatest in eastern Texas extending north through Missouri, the Southeast around Atlanta, the Ohio River Valley, the Northeast, and the northwest Pacific Coast. The most significant measurement gaps occur in Oregon, Nevada, and California (except for the San Francisco Bay and Las Vegas areas), Florida, the Mid-Atlantic, across large portions of Canada, and a broad swath extending from the Rocky Mountains through the Upper Great Plains.

https://doi.org/10.5194/egusphere-2026-6663
Preprint. Discussion started: 16 November 2026
© Author(s) 2026. CC BY 4.0 License.

Pollen Sense has been evaluated against traditional pollen counting methods in a number of recent studies (Buters et al., 2024; Farooq et al., 2025; Jiang et al., 2022; Lucas and Bunderson, 2024; Maya-Manzano et al., 2023; Zhang et al., 2026). Most recently, Zhang et al. (2026) used a high-density Pollen Sense network to evaluate a predictive pollen model over the greater Atlanta area, demonstrating the utility of the network for model verification at local-to-regional scales. In some regions and studies, the sensors identify some taxa with better skill than others (e.g., successfully identifying tree pollen but some difficulty with grass and weed pollen in the southeast US; Jiang et al., 2022). In general, these assessments find that Pollen Sense sensors capture the timing and variability of pollen seasons well while often exhibiting larger discrepancies in magnitude relative to manual counts. This is especially true for grouped taxa like trees, which exhibit significant uncertainty in some studies (e.g., Maya-Manzano et al., 2023). This distinction is relevant to our model evaluation, which prioritizes temporal correlation and phenological timing over magnitude. The Pollen Sense classifier is retrained continuously as its image library expands, and as such, the algorithm and training-set size in the present study exceed those evaluated in some earlier studies. Critically, the Pollen Sense network offers a novel, automated, and ever-expanding network that provides data in near-real-time that can be used for forecast verification.

2.2 PECM

We use the PECM v2.0 (Wozniak and Steiner, 2017; Zhang and Steiner, 2022) to produce pollen emission estimates over our study domain. PECM uses the distribution of the 13 pollen-emitting taxa shown to account for 77% of the total pollen across the United States from 2003–2010, which include: nine taxa of deciduous broadleaf trees (DBF, *Acer*/maple, *Alnus*/alder, *Betula*/birch, *Fraxinus*/ash, *Morus*/mulberry, *Platanus*/plane, *Populus*/poplar, *Quercus*/oak, *Ulmus*/elm), two evergreen needleleaf trees (ENF, including Cupressaceae/cypress, *Pinaceae*/pine), grasses (Poaceae; C3, C4), and one type of weed (*Ambrosia*/ragweed). PECMv2.0 uses empirical relationships between the previous year's annual average temperature and observed surface pollen counts to develop season start and end dates, generating emission potentials (grains m^{-2} d^{-1}) for each day and grid point for the 13 taxa.

Previous studies using PECM used the Biogenic Emission Land Database version 3 (BELD3) to provide the distribution of over 200 tree types across the United States at a horizontal resolution of 12 km. For this work, we have updated the PECM inputs to include version 6 of BELD, which was designed for the Biogenic Emission Inventory System version 4 (BEIS4; https://www.epa.gov/air-emissions-modeling/biogenic-emission-inventory-system-beis). The BELD6 product is offered at a resolution of 4 km and has been updated to include new land surveys that now includes Canada and Mexico. The updated dataset significantly increases the domain size and level of detail for the distribution of tree species. Figure S2 shows the fractional distribution of the 11 tree taxa (and their sum) used in the PECM as summed from the species listed in Wozniak and Steiner (2017). Figure S2 can be compared to Fig. 3 in Wozniak and Steiner (2017), which shows the same 11 fractional distributions but for the BELD3 dataset.

To obtain emission estimates of grass and ragweed pollen, we use the 0.05° (4.3 km at 40° N) PFT spatial distributions of grasses, crops, and urban locations from the Community Land Model dataset as implemented in the Model of Emissions of

https://doi.org/10.5194/egusphere-2026-6663
Preprint. Discussion started: 16 November 2026
© Author(s) 2026. CC BY 4.0 License.

Gases and Aerosols from Nature (MEGAN)(https://bai.ess.uci.edu/megan/data-and-code/megan21)(Fig. S3). The BELD6 dataset also includes crop distribution (Fig. S3d), yet we use the CLM data to differentiate between C3 and C4 grass distributions, which have different seasonal emission patterns. Monthly average 2 m temperature is taken from NOAA/NCEP GHCN CAMS (https://psl.noaa.gov/data/gridded/data.ghcncams.html) at 0.5° resolution. The CAMS temperature and the CLM urban, crop, and grass distributions are mapped to the BELD6 4 km domain using 1st order conservative mapping with ESMF. The PECM emission potentials are then generated on the BELD6 domain, and we regrid these emissions (summed tree, summed grass, ragweed) to the RAP-Chem model domain using ESMF with 1st order conservative mapping.

Actual pollen emissions are calculated online (i.e., at each model time step) by modifying the PECM emission potentials using functions involving the RAP-Chem-simulated downward shortwave radiation, wind speed, relative humidity, and precipitation (Wozniak and Steiner, 2017). Emissions are converted from grains m^{-2} d^{-1} to mass mixing ratios using the diameters and densities in Table 1. Multiple genera are lumped together for both tree and grass pollen emissions (weed pollen only represents ragweed), and there are large variations in pollen size between lumped species, e.g., Oak ~25 µm; Pine ~70 µm. The lumped grain diameters in Table 1 therefore misrepresent the emitted mass, and so also the physics processes that depend on size (see Sect. 2.4 and Sect. 4).

Table 1. Pollen tracers added to RAP-Chem

Species	*Name in code*	*Diameter (µm)*	*Density (kg m^{-3})*	*Refractive Index*[a]	*Wet Scav. Coef.*
Intact Tree Pollen	polp_tree	20.0	1200	1.53 + 0.0*i*	0.5
Intact Grass Pollen	polp_grass	20.0	1200	1.53 + 0.0*i*	0.5
Intact Weed Pollen	polp_weed	20.0	1200	1.53 + 0.0*i*	0.5
Lump Ruptured Pollen	pols_all	0.15	1425	1.53 + 0.0*i*	0.5
Total Intact Pollen[b]	polp_all	20.0	1200	1.53 + 0.0*i*	0.5

[a]*The current framework enables both short and longwave radiation interactions using optical properties calculated online using Mie theory under the assumption of homogeneous mixing. Values follow that used for organic carbon in WRF-Chem*
[b]*Only simulated prior to 15 March 2025*

SPP are formed in the atmosphere when intact pollen ruptures due to either osmotic or electrical stress; i.e., when relative humidity exceeds 80% or in the presence of lightning (Subba et al., 2023). When this occurs, 70% of intact pollen is converted to SPP for humidity-induced rupture, 10% for lightning-induced rupture. This mechanism is highly uncertain and likely contributes to the biases found when evaluating RAP-Chem against observations (Sect. 3).

2.3 RAP-Chem

The RAP-Chem (Schnell et al., 2026) is a version of the Rapid-Refresh (RAP), which is based on the WRF version 3.9 with significant modifications to the physics and dynamics packages (Benjamin et al., 2016). The experimental RAP-Chem forecast (https://rapidrefresh.noaa.gov/RAPchem/) ran at NOAA GSL starting August 2020, with the first pollen forecasts

https://doi.org/10.5194/egusphere-2026-6663
Preprint. Discussion started: 16 November 2026
© Author(s) 2026. CC BY 4.0 License.

integrated in 2022. The experiments herein use the source code and static fields as of the 15 March 2025 06Z forecast. An error was found in the 2025 emissions generated for the real-time RAP-Chem, which resulted in zero emissions from C4 grasses after September 1. We note this difference below when discussing the forecast skill. RAP-Chem is run with 51 vertical levels from the surface to 10 hPa at a 13.5 km horizontal resolution over a domain that includes North and Central America, as well as parts of South America, Europe, and Asia. The lowest model layer is ~16 m thick, with the first ~8 layers in the lowest 1 km of the atmosphere. An important consideration is that the operational RAP(-Smoke) undergoes extensive data assimilation (Benjamin et al., 2016) and the real-time RAP-Chem utilizes the assimilated input and boundary conditions. Chemical boundary conditions come from the default WRF-Chem profiles. Total ozone columns are provided by the Global Forecast System v16 (GFS, https://www.nco.ncep.noaa.gov/pmb/products/gfs/). The model physics options include the Thompson-Eidhammer microphysics scheme (Thompson and Eidhammer, 2014), the Grell-Freitas cumulus scheme (Freitas et al., 2021) with convective removal and parameterized aqueous chemistry (Li et al., 2018), the Mellor–Yamada–Nakanishi–Niino eddy diffusivity mass-flux (MYNN-EDMF; Olson et al., 2026) boundary layer and surface layer schemes with modifications (Schnell et al., 2026), and the Rapid Update Cycle (RUC) land model (Smirnova et al., 2016). For radiation, we use the Rapid Radiative Transfer Model for GCMs (RRTMG; Clough et al., 2005) for both shortwave and longwave radiation schemes and improve physics coupling by supplying RRTMG with prognostic ozone profiles. Resolved wet deposition occurs via the *wetdep_ls* WRF-Chem module. For code simplicity, pollen aerosols are embedded in the Modal Aerosol Dynamics Model for Europe with Volatility Basis Set (MADE-VBS) aerosol module (Ahmadov et al., 2012). This primarily couples the emission, dry deposition, rupture mechanisms, and total $PM_{2.5}$ and PM_{10} calculations (i.e., pollen is not dynamic between Aitken and accumulation modes and has no connection to the VBS routines). Pollen is emitted in the lowest model layer (see Sect 4). The RAP-Chem simulations incorrectly did not include gravitational settling of coarse pollen aerosols, for which the implications are discussed in Sect. 2.4 and Sect. 4.

Accurately capturing the impact of meteorology on pollen emissions depends first on an accurate meteorological forecast. As described in Sect. 2.2, the emissions of pollen in the model heavily depend on the model-simulated wind speed, relative humidity, and precipitation. The RAP-Chem uses the initial and boundary meteorological conditions from the operational RAP forecast model, which has been extensively evaluated for its skill in numerical weather prediction (e.g., Benjamin et al., 2016).

2.4 Data post-processing, filtering, and phenological metric calculations

For direct comparison to the NAB and Pollen Sense observations, mass mixing ratios ($\mu g\ kg^{-1}$) of RAP-Chem simulated tree, grass, and weed pollen are converted to grains m^{-3} using the diameters and densities listed in Table 1. The same values are used to convert PECM emissions in grains $m^{-2}\ d^{-1}$ to mass mixing ratios in RAP-Chem (Sect. 2.2). Because the RAP-Chem is an experimental forecast model, there are several days during 2025 when the forecast did not run (e.g., HPC cluster maintenance). Typically, the RAP-Chem provides a 48 h forecast, which we use to gap-fill missing hours when possible (i.e., the 24–48 h forecast output from the preceding day's forecast is used for the current day). Daily mean RAP-Chem

https://doi.org/10.5194/egusphere-2026-6663
Preprint. Discussion started: 16 November 2026
© Author(s) 2026. CC BY 4.0 License.

concentrations were subsequently computed only when a minimum of 18 out of 24 hourly outputs were available. Days failing this completeness threshold (N = 20 d) were treated as missing. Prior to 15 March 2025, the RAP-Chem only included a single bulk total pollen tracer rather than explicitly speciated tree, grass, weed categories. For the analysis during this early-season period, bulk/total pollen concentrations are partitioned into tree, grass, and weed using local daily emission fractions derived from the PECM emission potentials (see Sect. 2.2). Where PECM emission potentials are zero (i.e., all simulated pollen is transported) we use the average over an 11 x 11 grid cell box (~150 km). If this box-average is still zero we use the domain average. To compare RAP-Chem against Pollen Sense at the grid cell level, daily RAP-Chem values are linearly interpolated to the 30 km Pollen Sense grid. Pollen Sense total pollen is calculated as the sum of tree, grass, and weed pollen rather than using the total pollen product. Pollen Sense tree pollen is anomalously high across much of North America from 1 to 19 January 2025 and abruptly decreases on 20 January. These likely interpolated winter values result in a prematurely early Pollen Sense tree season (see below) in these locations (Fig. S1). For direct comparisons to the NAB sites, observations are colocated to the RAP-Chem and Pollen Sense grids using a cosine-latitude-weighted Euclidean distance. The NAB time series are filled with zeros before the first and after the last measurement. Means, biases, and phenological indicators are then calculated over valid values. Correlation calculations do not use the zero-filled time series, and we do not plot them in the time series (Fig. 2). We also apply a one-day lag to the comparisons (i.e., January 2 NAB "observations" are compared to January 1 RAP-Chem and Pollen Sense values). For our primary analysis, results are calculated using the daily unsmoothed and unfiltered time series, but we also perform a secondary analysis in some instances where we remove pollen concentrations in all datasets that are less than 0.05 grains m^{-3} and smooth the time series with a five-day centered rolling mean.

We extract phenological indicators (i.e., the day of year (DOY) of the start-of-season (SOS), peak-of-season (POS), and end-of-season (EOS)) at each NAB site and each grid cell of the RAP-Chem and Pollen Sense datasets. Phenology is not computed for the Springfield, MO site since data is only available for March–April. Phenology is computed only where at least ten days are available within the season (see below). For RAP-Chem, phenology is only computed where the annual PECM emission potential is nonzero (for Pollen Sense, at the nearest RAP-Chem grid cell). We relax this requirement at grid cells with NAB sites since observed pollen at these locations could reflect a source PECM misses, but that RAP-Chem could transport there (e.g., tree pollen at Boise, ID). We first fill gaps of up to five consecutive missing days with linear interpolation, and then smooth each of the time series using a five-day centered rolling mean requiring at least three valid days (Zhu et al., 2024) to account for data gaps and spurious daily values. Each phenological indicator is derived from these smoothed time series and constrained to biologically plausible windows. POS is defined by the maximum of the smoothed time series, with the tree and grass peak constrained to DOY = 1–199 and the weed peak constrained to DOY 183–365. SOS and EOS are constrained to DOY = 1–243 for tree pollen, DOY = 1–304 for grass pollen, and DOY = 183–365 for weed pollen. Both methods described below use these windows. Because we only evaluate RAP-Chem starting at the beginning of 2025, the seasonality of winter Cupressaceae pollen is unaccounted for and so the phenological indicators for trees represent the spring–summer season (e.g., Waco, TX). We calculate SOS and EOS using two separate methods. The first follows a

https://doi.org/10.5194/egusphere-2026-6663
Preprint. Discussion started: 16 November 2026
© Author(s) 2026. CC BY 4.0 License.

modified version of Wozniak and Steiner, (2017), who define SOS and EOS as the DOY when cumulative pollen concentrations are 2.5% (97.5%) of the total. We restrict this to the constrained season windows and instead choose a value of 5% (95%) but also compute SOS (EOS) using a value of 2.5% (97.5%) and 7.5% (92.5%) to capture uncertainty. The second method uses a fractional approach, where we step backward (forward) from POS, finding the last (first) DOY in the smoothed time series when the pollen concentrations on five consecutive valid days remain below 5% of the POS. We also calculate SOS and EOS using thresholds of 2.5% and 7.5% of the POS concentration to capture uncertainty. Where the series never remains below the threshold for a full five-day window within the season window, the boundary falls back to the pre-peak (SOS) or post-peak (EOS) minimum within the window (i.e., the day of lowest smoothed value on that side of the peak). The fractional method helps to eliminate the impact of pre- and post-season noise and considers missing data at the beginning and end of the time series. Our primary phenological indicator estimates are the mean of the two methods with error bars spanning both methods and the three thresholds.

Initial evaluations of RAP-Chem against NAB and Pollen Sense observations revealed grass and weed pollen concentrations were overestimated by nearly two orders of magnitude, while tree pollen at most NAB sites was within one order of magnitude. The discrepancies partly reflect a mismatch between emission heights, measurement heights, and the RAP-Chem's omission of gravitational settling. In the RAP-Chem configuration used here, intact pollen is considered a coarse-mode aerosol within the MADE-VBS module. Intact pollen undergoes surface dry deposition, whose velocity is set to the bulk coarse-mode value and is applied as a surface sink during vertical mixing (Schnell et al., 2026). However, the separate gravitational settling module (GOCART) was incorrectly omitted, and so pollen is removed only at the surface and does not fall through the atmospheric column. Tree pollen is both emitted and measured at an elevated height (~8 m, the center of the first model layer), and so the near-source vertical gradient is somewhat unaffected by this omission. Conversely, grass and weed pollen are emitted at <1 m but measured aloft (Rojo et al., 2019), missing the significant gravitational settling that impacts vertical concentration gradients (Damialis et al., 2017). Consequently, post-processing corrections were only applied to grass and weed pollen. The correction (α) follows a steady-state surface layer balance using the ratio of settling-corrected to settling-uncorrected concentrations is (Eq. 1)

$$\alpha = \frac{V_d}{V_d + V_S}, \quad (1)$$

where V_S is the gravitational settling velocity and V_d the modeled (non-settling) surface removal velocity. We evaluate V_S from the Stokes–Cunningham expression used within the model at 20 °C and 1 atm (Eq. 2)

$$V_s = \frac{\rho g C_C D^2}{18\mu}, \quad (2)$$

where D = 20 µm, and ρ = 1200 kg m^{-3}, µ is the dynamic viscosity of air = 1.81 x 10^{-5} kg m^{-1} s^{-1}, C_C is the Cunningham slip correction factor = 1.008, and g is gravitational acceleration. This yields $V_S \approx 0.015$ m s^{-1}; combined with an a priori surface removal velocity $V_d \approx 2 \times 10^{-4}$ m s^{-1} (Seinfeld and Pandis, 2016; Zhang, 2001), α ≈ 0.0136 for grass and weed pollen, a ~74x reduction. As described above, tree pollen is assigned α = 1 (no reduction). Critically, V_d is taken from the literature rather than tuned to the observed bias, so α is an a priori adjustment. V_S is computed with a density of 1200 kg m^{-3}, consistent with

https://doi.org/10.5194/egusphere-2026-6663
Preprint. Discussion started: 16 November 2026
© Author(s) 2026. CC BY 4.0 License.

the grains-to-mass conversion in PECM-to-RAP-Chem emissions, rather than the incorrect value of 1500 kg m^{-3} internal to the RAP-Chem deposition scheme. Because V_d is prescribed a priori, this internal inconsistency does not propagate into the correction. Finally, because α is applied as a constant across the entire dataset, it only affects the magnitude (bias) comparisons and does not impact the seasonality and timing (i.e., SOS, POS, and EOS) and rank-correlation analyses that constitute our primary evaluation.

Because the grain rupture into SPP mechanisms used in the model are highly uncertain, we perform a separate analysis where SPP mass is reconstituted back into intact pollen in proportion to tree, grass, and weed pollen, and then converted to grains m^{-3} as above. We find that the Fisher z-averaged Spearman rank correlation of total pollen across the NAB sites is largest when all SPP mass is returned to intact pollen.

3 Results

3.1 PECM pollen emission potentials

Figure 1 shows the average daily pollen emission potentials (grains m^{-2} d^{-1}), for each season used in the 2025 forecasts (i.e., including the C4 grass bug). Here the term "emission potential" describes the output of PECM, which reflects the total potential for pollen emissions prior to accounting for online meteorology. Figure S4 shows the revised emission potentials after correcting the C4 grass error.

Total PECM pollen emission potentials in North America (NA) are dominated by trees, with many locations exceeding 1 million grains m^{-2} d^{-1}. A similar magnitude of emissions is maintained from April through July as the latitudinal emission peak moves northward. During spring (MAM, Fig. 1a–d), peak tree pollen emissions occur in the US northeast, southeast and high elevation locations in the West. Pollen emissions in Canada are even more so dominated by trees, reaching more than 10 million grains m^{-2} d^{-1} in several locations. Total tree pollen emissions are lowest in autumn months (SON) and have a pronounced bimodal latitudinal maximum. Winter months (DJF) have relatively strong tree pollen emissions in the southeast US and to a lesser extent, the West Coast. Grasses are always emitting pollen somewhere in NA with relatively consistent emissions throughout the year in the revised emission (Fig. S4). North American grass pollen emissions peak in June, with relative spatial peaks in the US West and the eastern US from ~40° N–45° N. The spring grass pollen emission peak is similar in magnitude to summer, with the highest emissions in the southern Mississippi River Valley and Mexico. Several regions (e.g., Pacific Northwest, CA, SE) experience grass pollen emissions throughout the year, while other locations (e.g., NE) have a much shorter grass season (April–Aug). The ragweed emission season doesn't typically begin until mid-summer in most locations, with the latitudinal maximum marching southward through autumn. Seasonally, total North American ragweed pollen emissions reach a maximum in September, with the largest emissions in the central US and the interior of the Pacific Northwest.

https://doi.org/10.5194/egusphere-2026-6663
Preprint. Discussion started: 16 November 2026
© Author(s) 2026. CC BY 4.0 License.

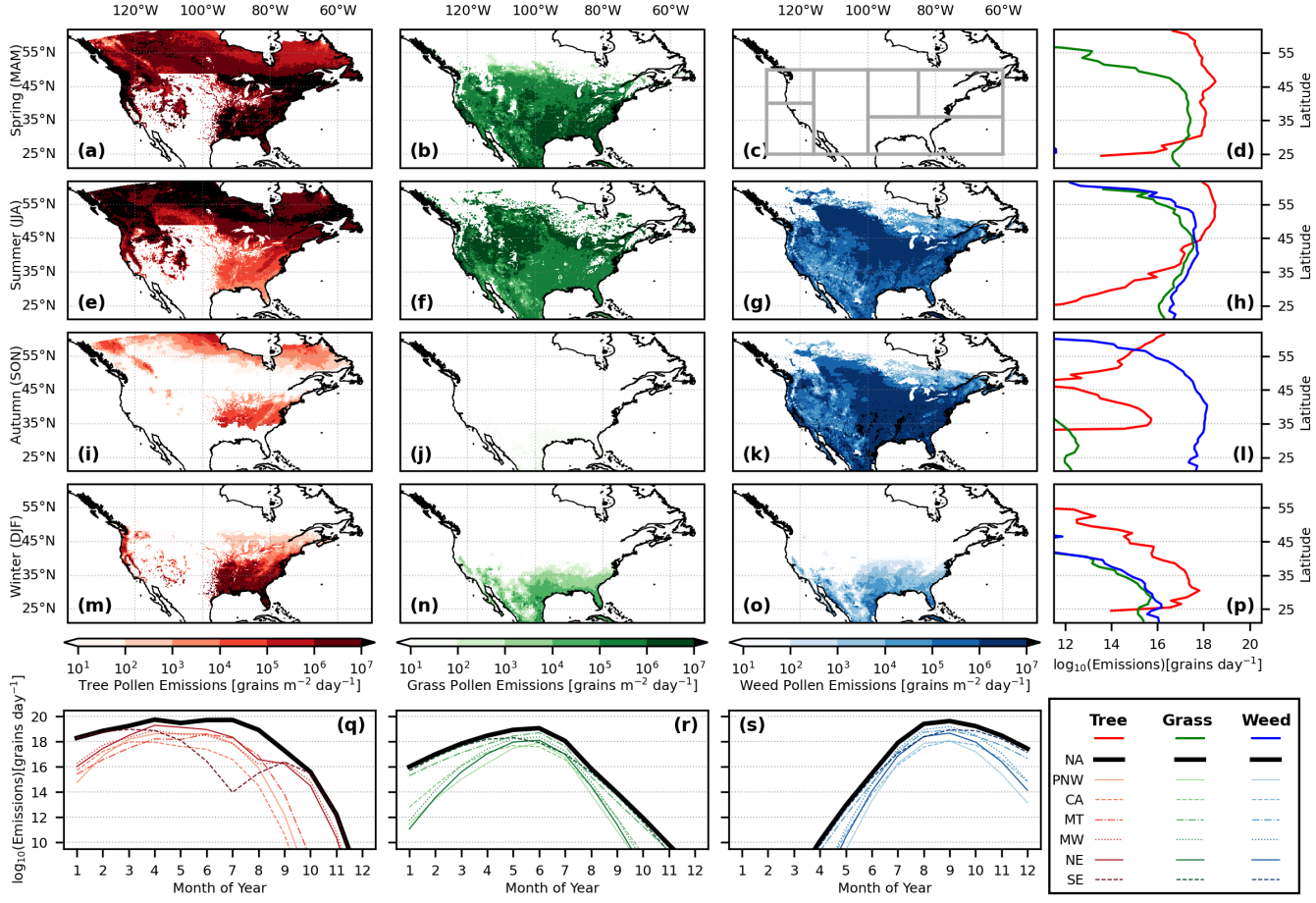
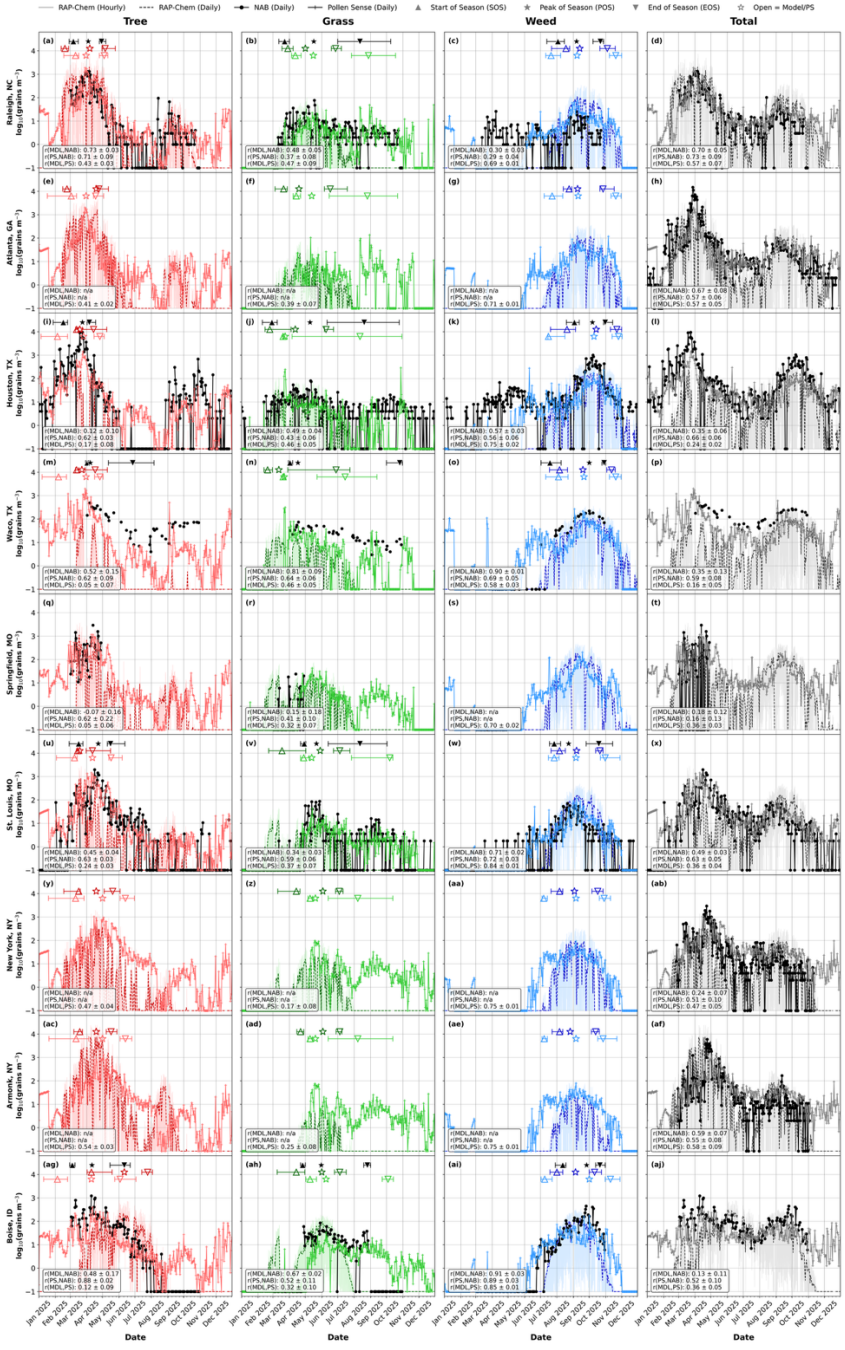


Figure 1. Average daily PECM calculated pollen emission potentials (grains m^{-2} d^{-1}) for tree (**a**,**e**,**i**,**m**,**q**), grass (**b**,**f**,**j**,**n**,**r**), and weed (**c**,**g**,**k**,**o**,**s**) pollen for (**a**–**d**) MAM, (**e**–**h**) JJA, (**i**–**l**) SON, and (**m**–**p**) DJF for 2025. (**d**,**h**,**l**,**p**) Seasonal average daily emissions summed over each 1° latitude bin (grains d^{-1}). (**q**,**r**,**s**) is the monthly summed annual cycle (grains d^{-1}). Regions loosely follow Wozniak and Steiner, (2017): 'PNW','CA', 'MT', 'MW', 'NE', 'SE' have minimum/maximum latitudes of 40°/50°, 25°/40°, 25°/50°, 36°/50°, 36°/50°, and 25°/36° and minimum/maximum longitudes of 130°/116°, 130°/116°, 116°/100°, 100°/85°, 85°/60°, and 100°/60° and are shown in (**c**). 'NA' is the values over North America.

3.2 Comparisons with NAB sites

Figure 2 shows the 1 January – 31 December 2025 time series of daily averaged tree, grass, weed, and/or total pollen concentrations (grains m^{-3}) at each of the NAB sites in Table S1. We also plot the daily averaged Pollen Sense and hourly and daily averaged RAP-Chem time series over the grid cells corresponding to the NAB sites. While we cannot compare higher frequency model output (i.e., hourly) to the observations, the average diurnal cycle of RAP-Chem simulated tree, grass, weed, and total pollen at each NAB site is shown in Fig. S5, showing that in general, simulated maximum concentrations occur in the late afternoon (~1:00–3:00 PM LST). We calculate the Spearman rank correlations (r) across each dataset (Fig. 2–3; Tables 2, S3–S6) and use the Spearman correlation over Pearson due to outliers in the pollen time series. The standard deviation of r at each location in Fig. 2 is calculated over temporal lags of ±14 d. Each plot also

https://doi.org/10.5194/egusphere-2026-6663
Preprint. Discussion started: 16 November 2026
© Author(s) 2026. CC BY 4.0 License.



335

Figure 2. Time series of 2025 tree, grass, weed, and total pollen concentration (columns, left-to-right, $\log_{10}$(grains m^{-3})) over each NAB site (rows; daily, black), the 30 km Pollen Sense grid cell containing the site (daily, solid, plusses), and the 13.5 km RAP-Chem grid cell (hourly: solid, no markers; daily: dashed, no markers). Spearman rank correlations (r) ± the standard deviation of r across temporal lags of ±14 d are shown for each site. SOS, POS, and EOS are denoted by upward triangles, stars, and downward triangles, respectively.
340 Phenology is not calculated for Springfield, MO. The central estimate is the average of the cumulative and fractional methods with the range spanning the values across both methods and three thresholds. Values below 10^{-1} grains m^{-3} (including NAB counts of 0) are plotted at 10^{-1}. RAP-Chem grass and weed pollen are scaled by $\alpha = 0.0136$.

https://doi.org/10.5194/egusphere-2026-6663
Preprint. Discussion started: 16 November 2026
© Author(s) 2026. CC BY 4.0 License.

denotes the central estimate and range of SOS, POS, and EOS of each dataset across the two methods and their three thresholds (see Sect. 2.4). The values calculated for the different methods are summarized and compared in Fig. S6. Figure 3 shows tree, grass, weed, and total pollen averaged over each grid cell in the Pollen Sense and RAP-Chem datasets, as well as the bias (grains m^{-3}, RAP-Chem minus Pollen Sense) and *r* over the full domain. Fig. S7 and Fig. S8 show the monthly spatial averages of tree, grass, weed, and total pollen for Pollen Sense and RAP-Chem, respectively, with the corresponding values of the NAB stations overlaid on the maps. Tables S3–S5 summarize the means, correlations, and phenological metrics across each of the sites in Table S1 and regions listed in Fig. 1 for the three datasets.

Comparing first the NAB observations to the Pollen Sense product shows that Pollen Sense reproduces most of the individual pollen groups (i.e., tree, grass, weed) and total pollen time series at each of the NAB sites with moderate skill (Tables 2, S3–S5) even though the Pollen Sense grid cell may not actually contain a sensor (i.e., it may be an interpolated value or may be up to 30 km away from the NAB sensor even when located inside the grid cell). The Pollen Sense average *r* (Fisher's z-transformed) across the NAB sites is 0.70, 0.50, 0.67, and 0.56 for tree, grass, weed, and total pollen respectively (Table 2). For individual sites, the highest *r* occur for tree and weed pollen at Boise, ID (0.88 and 0.89, respectively) and are lowest for weed and grass pollen at Raleigh, NC (0.29 and 0.37, respectively) and total pollen at Springfield, MO (0.16), with all other pollen type-site correlations exceeding 0.4 (Fig. 2; Tables S3–S5). Pollen Sense annual mean tree pollen is biased high compared to NAB at four of six tree-reporting sites (mean bias (MB) = -27.9 grains m^{-3}, median bias = 13.7 grains m^{-3}); grass pollen is biased low at four of six grass-reporting sites (MB = -0.4 grains m^{-3}, median bias = -1.1 grains m^{-3}); and weed pollen is biased high at three of five weed-reporting sites (MB = -4.2 grains m^{-3}, median bias = 2.6 grains m^{-3})(Tables S3–S5).

Pollen Sense also captures the phenology for most site–taxa combinations (Fig. 2, Fig. S6; Tables S3–S5). Springfield, MO phenology is excluded since the time series is too short to calculate meaningful indicators. Pollen Sense SOS for tree, grass, and weed pollen have mean absolute errors (MAE) of 21.0 d, 13.9 d, and 22.4 d, respectively. Of the indicators, POS is generally best captured, with MAE = 5.2 d, 18.4 d , and 6.6 d, for tree, grass, and weed, respectively. EOS is captured with similar skill to tree and weed SOS (MAE = 19.2 d, 44.2 d, and 21.4 d, for tree, grass, and weed, respectively), though it is also the least constrained, especially for grass (Fig. S6). For tree pollen, Pollen Sense is early at four of five sites for SOS and POS and late at three of five sites for EOS. For grass pollen, Pollen Sense is late at three of five sites for SOS and EOS, and early at all but one site for POS. For weed pollen, Pollen Sense is early for SOS at three of five sites, late for POS at all but one site, and late for EOS at all sites. Overall, while there are discrepancies between NAB and Pollen Sense, we are comfortable using the Pollen Sense data to evaluate the RAP-Chem forecast in regions without NAB pollen counting sites, noting that forecast skill or deficiencies could be over- or underestimated.

Comparing RAP-Chem to NAB shows the model has less skill than Pollen Sense in reproducing the daily variations in total pollen ($r = 0.44$), with moderate skill for the individual types (tree (0.40) grass (0.53) and weed (0.74). The highest correlations are for tree pollen at Raleigh, NC (0.73), grass pollen at Waco, TX (0.81), weed pollen at Waco, TX (0.90), and weed pollen at Boise, ID (0.91). RAP-Chem correlations are lowest at Springfield, MO (tree = -0.07, grass = 0.15), though

https://doi.org/10.5194/egusphere-2026-6663
Preprint. Discussion started: 16 November 2026
© Author(s) 2026. CC BY 4.0 License.

the time series is very short so it may not be meaningful (this also impacts the across-site Fisher z averaged correlations). Tree pollen at Houston, TX is not well-captured when considering the full year (r = 0.12), however within-season (i.e., from SOS–EOS, "seas" in Table S3) correlations at both Texas sites are relatively high (Houston, TX = 0.69; Waco, TX = 0.72). RAP-Chem biases at the TX sites are large however, with in-season mean tree pollen underestimated by a factor of ~125 at Houston, TX (14.4 grains m^{-3} vs. 1806.2 grains m^{-3}) and ~60 at Waco, TX (3.2 grains m^{-3} vs. 193.6 grains m^{-3}). Pollen Sense underestimates in-season Houston, TX tree pollen by only ~6x, indicating a bias in PECM-RAP-Chem rather than conflicting observations. Interestingly, correlations for total pollen are consistently lower than grass and weed pollen due to compensating biases and variations in the dominant pollen type, namely the influence of tree pollen. This is important to consider when evaluating any forecast model for its accuracy as it may be that errors in one type of pollen caused the mismatch. The full-year correlation largely reflects capturing the overall timing of the pollen season rather than day-to-day variability within it. Correlations are calculated over the NAB-defined SOS–EOS (Tables S3–S5) reveals RAP-Chem skill drops substantially at several sites; for example, tree pollen r at Raleigh, NC falls from 0.73 to −0.19 and weed pollen at Boise, ID from 0.91 to 0.13. This full year vs. in-season mismatch in correlation is also seen in Pollen Sense at some sites (e.g., weed pollen r at Boise, ID drops from 0.89 to 0.05 and St. Louis, MO from 0.72 to 0.07). Within the season, Pollen Sense better captures tree pollen at NAB sites compared to RAP-Chem (r = 0.46–0.88 vs. −0.19–0.72; Table S3), while RAP-Chem better captures grass pollen (r = 0.33–0.81 for RAP-Chem, r = 0.19–0.65 for Pollen Sense; Table S4). In-season weed pollen correlations are similar (r = 0.05–0.72 for Pollen Sense, r = 0.13–0.67 for RAP-Chem; Table S5). Temporal smoothing (five-day, Sect. 2.4) improves RAP-Chem agreement with Pollen Sense for tree, grass, and total pollen substantially (e.g., tree pollen r increases from 0.29 to 0.67; grass pollen r from 0.36 to 0.60, and total pollen r from 0.42 to 0.57; Table 2), demonstrating RAP-Chem skill at capturing multi-day pollen episodes with less skill for high-frequency daily variability. Table S6 shows the correlations calculated with all SPP reconstituted back into intact pollen. Correlations change only slightly (≤ 0.02), indicating that the rupture parameterization is not a substantial source of bias in capturing timing. At most NAB sites, RAP-Chem is biased low in spring (summer) due to underestimated tree (grass) pollen and biased high in the fall due to overestimated weed pollen (Fig. S8). RAP-Chem and Pollen Sense agree with one another moderately well at the NAB site locations, with 16 of 27 tree, grass, and weed site correlations greater than 0.4 (20 of 27 greater than 0.3; Fig. 2; Tables S3–S5). The greatest agreement between RAP-Chem and Pollen Sense is found for weed pollen (r = 0.58–0.85). These generally high weed pollen correlations may reflect that ragweed is the only species accounted for in the RAP-Chem and so inter-species phase-shifts do not impact correlations (although Pollen Sense identifies other, less prominent weed types). Additionally, the unique shape and ubiquity of ragweed may be more readily detected by the updated Pollen Sense optical algorithm. Jiang et al. (2022), however, noted improvements were necessary for the Pollen Sense weed algorithm. RAP-Chem phenological indicator skill compared to Pollen Sense is slightly mixed. For tree pollen, RAP-Chem MAE = 19.9 d, 24.0 d, and 32.8 d for SOS, POS, and EOS, respectively; MAE = 20.7 d, 17.6 d, and 65.2 d for grass pollen; and MAE = 13.8 d, 12.2 d, and 12.2 d for weed pollen. For tree pollen, RAP-Chem is early for SOS and POS at three of five sites, and late for EOS at three of five sites. The largest tree errors are at Boise, ID, where the PECM-RAP-Chem grid cell

https://doi.org/10.5194/egusphere-2026-6663
Preprint. Discussion started: 16 November 2026
© Author(s) 2026. CC BY 4.0 License.

has no tree emissions and so simulated tree pollen is due to transport from surrounding forests. For grass pollen, SOS is early at four of five sites, POS is early at three of five sites, and EOS early at all five. The EOS bias is partly explained by the C4 grass emission error (Sect. 3.3). RAP-Chem weed phenological indicators are matched best; SOS and POS are late at three of five sites, and EOS is late at all sites except Boise, ID.

Table 2. Fisher z-averaged mean ± standard deviation of the Spearman rank correlations across the NAB sites for NAB vs. RAP-Chem, NAB vs. Pollen Sense, and Pollen Sense vs. RAP-Chem. Correlations in parentheses are calculated by smoothing each time series by a 5-day centered rolling average and dropping pollen counts < 0.05 grains m^{-3}.

Category	NAB vs. RAP-Chem	NAB vs. Pollen Sense	Pollen Sense vs. RAP-Chem
Tree	0.40 ± 0.27 (0.47 ± 0.41)	0.70 ± 0.10 (0.75 ± 0.10)	0.29 ± 0.18 (0.67 ± 0.15)
Grass	0.53 ± 0.21 (0.54 ± 0.37)	0.50 ± 0.10 (0.52 ± 0.13)	0.36 ± 0.10 (0.60 ± 0.10)
Weed	0.74 ± 0.23 (0.76 ± 0.11)	0.67 ± 0.20 (0.61 ± 0.12)	0.75 ± 0.08 (0.77 ± 0.08)
Total	0.44 ± 0.20 (0.55 ± 0.27)	0.56 ± 0.15 (0.73 ± 0.09)	0.42 ± 0.14 (0.57 ± 0.19)

3.3 RAP-Chem and Pollen Sense comparison over North America

Pollen Sense (Fig. 3d) shows the largest average daily total pollen concentrations from in the lower Mississippi River Valley and Gulf Coast, and California. RAP-Chem (Fig. 3h) total pollen is highest across the eastern US, the Pacific Northwest, and Canada (i.e., in heavily forested regions). RAP-Chem total pollen is biased high (>200 grains m^{-3}) relative to Pollen Sense in these forested regions. RAP-Chem total pollen is also biased high in east Texas and much of the east coast and low in the lower Mississippi River Valley and much of the West, Central, and Upper Midwest US (Fig. 3l) due to underestimated tree pollen. Correlations (Fig. 3p) are highest (~0.4–0.6) along the East Coast and a strip from Minnesota to Maine. The lowest correlations occur throughout the western US, though the spatial density of Pollen Sense monitors is very low in this area (<1 monitor per 10^5 km^2) and so the low correlations may simply be a result of interpolation artifacts of the Pollen Sense monitors to the 30 km grid.

Tree pollen concentrations in Pollen Sense (Fig. 3a) are highest in the lower Mississippi River Valley (>200 grains m^{-3}) and are also elevated throughout the central US, the Southeast, and the East Coast. RAP-Chem (Fig. 3e) tree pollen is greater than 200 grains m^{-3} across much of the eastern US, and greater than 500 grains m^{-3} in the Pacific Northwest and Canada, much higher compared to Pollen Sense (Fig. 3i). Tree pollen is biased low through the lower Mississippi River Valley, where Pollen Sense tree pollen is highest. These biases likely reflect a combination of omitted gravitational settling and uncertainties in the PECM emission potentials. Pollen Sense values in sparsely monitored, heavily forested regions are likely biased low due to interpolation from sensors with lower tree pollen. The correlation map for tree pollen (Fig. 3m) shows a band of moderate correlation from the Gulf Coast up through the Mid-Atlantic and weak correlations dominating the western half of the US. Grass pollen is underestimated slightly in most locations, generally biased low throughout the eastern half of the US and the Southeast, with positive biases in parts of the desert Southwest (Fig. 3j). As noted in Sect. 2.3, an error in the experimental

https://doi.org/10.5194/egusphere-2026-6663
Preprint. Discussion started: 16 November 2026
© Author(s) 2026. CC BY 4.0 License.

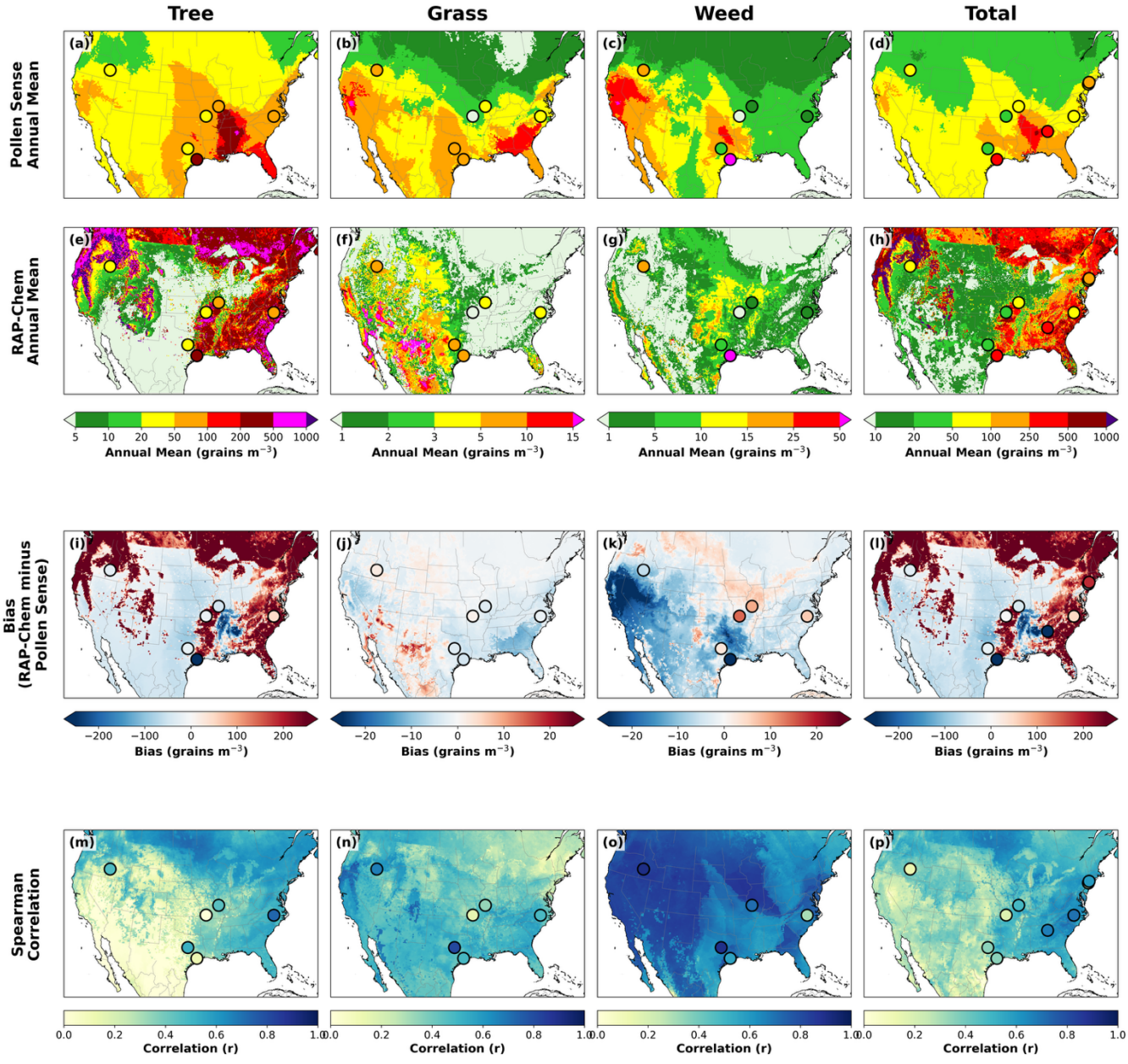


Figure 3. Average of 1 Jan – 31 Dec 2025 concentrations of Pollen Sense (**a**–**d**) and RAP-Chem (**e**–**h**) for tree (column 1), grass (column 2), weed (column 3), and total pollen (column 4) overlaid with NAB concentrations (dots). (**i**–**l**) Mean bias (grains m^{-3}) and (**m**–**p**) Spearman rank correlations. NAB averages are calculated over the full year (i.e., including 0's, NaN) and the bias is shown with respect to RAP-Chem. Correlations are calculated with respect to RAP-Chem over days with available NAB observations. RAP-Chem grass and weed pollen are scaled by $\alpha = 0.0136$.

forecast resulted in zero emissions from C4 grasses after September 1. This omission impacts regions dominated by warm season C4 grasses such as the southern and central US. In these regions RAP-Chem has a pronounced negative bias in grass pollen concentrations during the autumn months compared to both NAB (Fig. S8) and Pollen Sense observations (Fig.

https://doi.org/10.5194/egusphere-2026-6663
Preprint. Discussion started: 16 November 2026
© Author(s) 2026. CC BY 4.0 License.

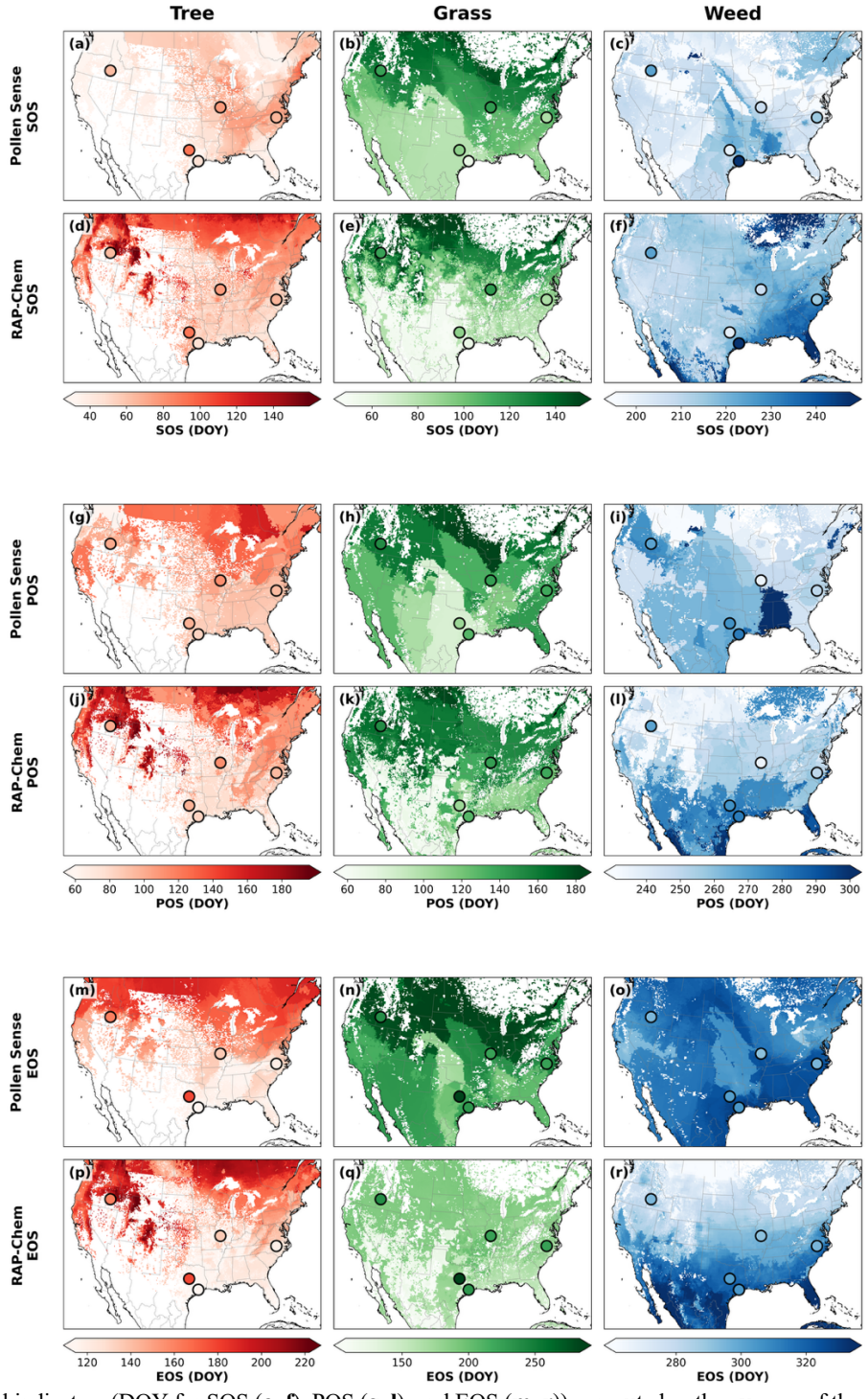


Figure 4. Phenological indicators (DOY for SOS (**a**–**f**), POS (**g**–**l**), and EOS (**m**–**r**)) computed as the average of the cumulative and fractional methods across North America. Columns show from left to right tree, grass, and weed pollen. Pollen Sense (**a**–**c**, **g**–**i**, **m**–**o**) and RAP-Chem (**d**–**f**, **j**–**l**, **p**–**r**) are shown on alternating rows, with NAB sites as filled circles. Color scales span the 5th–95th percentiles of the combined Pollen Sense and RAP-Chem values.

https://doi.org/10.5194/egusphere-2026-6663
Preprint. Discussion started: 16 November 2026
© Author(s) 2026. CC BY 4.0 License.

S7), which can also be seen to a lesser extent in the annual bias (Fig. 3j). The resulting overall correlation for grass pollen (Fig. 3n) shows moderate agreement (r ~ 0.3–0.6) over most of the domain, with a band that stretches southeast from the Pacific Northwest through Colorado and parts of California. Correlations are much lower throughout eastern Canada and the northeast US.

Weed pollen follows a similar trend as tree and grass pollen, with RAP-Chem underestimations in most locations. The highest average weed pollen in Pollen Sense (>25 grains m^{-3}) is found across the northern half California and its downwind neighbors to the east as well as a small region along the Texas-Oklahoma border (Fig. 3c). RAP-Chem weed pollen is highest in California and the central US (Fig. 3g), but is biased low compared to Pollen Sense through most of the West, and the lower Mississippi River Valley (Fig. 3k). In Sect. 3.2 we found that RAP-Chem and Pollen Sense weed pollen was in best agreement at the NAB site locations. The same is true for the full North American analysis (Fig. 3o), with many locations' correlations, particularly throughout the West and Midwest, exceeding 0.80.

Phenological indicators across North America are shown in Fig. 4 and summarized in Tables S3-S5 and Table S7. For tree pollen, domain-wide spatial correlations for SOS, POS, and EOS are -0.21, 0.15, and 0.60, respectively. SOS is mostly earlier in Pollen Sense and earliest compared to RAP-Chem throughout mountainous regions and Canada (45–65 days in PNW, CA, and MT; Table S3). POS and EOS are more comparable between RAP-Chem and Pollen Sense, though Pollen Sense is still earlier for both metrics in large portions of the domain. POS is within one week in three regions (CA, NE, and SE) and EOS is within nine days in PNW, MW, NE, and SE (Table S3). Across regions, tree phenology in the SE (65.6%, 68.8%, and 70.4% of SOS, POS, and EOS matched within 14 days) is arguably the best simulated.

Patterns are matched best for grass pollen, with domain-wide spatial correlations for SOS, POS, and EOS of 0.83, 0.66, and 0.58, respectively. Pollen Sense has generally later metrics and is especially pronounced for EOS due to the C4 grass emission error in RAP-Chem. SOS is within two weeks in PNW, CA, and the NE; POS is within one week in PNW, CA, MW, and NE; and EOS is expectedly biased by 45–89 d across regions (Table S4).

Weed pollen indicators are generally matched best in terms of magnitude, though domain-wide spatial correlations for SOS, POS, and EOS of 0.09, 0.31, and 0.11, respectively are generally lower than grass and tree pollen (except tree pollen SOS and POS). SOS is within 16 d in all regions; POS is within one week in all but the PNW (21-day separation); and EOS is later in Pollen Sense in all regions by 5–30 days (Table S5).

4 Conclusions and discussion

Here we have presented the first comprehensive evaluation of the experimental Rapid-Refresh model coupled to Chemistry (RAP-Chem) for forecasting speciated (tree, grass, and weed) airborne pollen across North America for the 2025 calendar year. By coupling the Pollen Emissions for Climate Models (PECM v2.0) with a high-resolution coupled chemistry-meteorological model, we have moved beyond empirical, point-based statistical forecasts often used in the private sector to a forecast that include emissions coupled to model simulated meteorology, horizontal transport, vertical mixing, intact pollen

https://doi.org/10.5194/egusphere-2026-6663
Preprint. Discussion started: 16 November 2026
© Author(s) 2026. CC BY 4.0 License.

grain rupture into SPP, physics-based representations of loss processes (i.e., wet scavenging, dry deposition, rupture), and physics interactions (i.e., radiation). We have evaluated the model against both manual counts from AAAAI NAB sites as well as an interpolated (30 km) product of automated sensor observations from the Pollen Sense network.

A critical finding is the viability of Pollen Sense to supplement the relatively sparse NAB pollen monitoring sites. Despite relying on interpolated data in some regions, the Pollen Sense network demonstrated skill in reproducing the daily variations and phenological timing (start, peak, and end of season; SOS, POS, and EOS, respectively) of individual pollen types observed by NAB stations, providing a foundation for assessing RAP-Chem's skill outside the NAB sites. Given the lack of a federally-operated or partnered, high-density pollen monitoring network in the United States, integrating private sector automated sensors is a highly promising pathway to evaluate and constrain regional atmospheric models of airborne pollen.

The RAP-Chem demonstrated encouraging skill in capturing salient features of pollen concentrations, though still with ample shortcomings. Weed pollen was simulated most successfully, followed by grass pollen and tree pollen. For weed and grass pollen, RAP-Chem's overall agreement (Spearman rank correlation, r) with NAB was similar to that of Pollen Sense, while tree pollen was less successfully simulated (r = 0.40 vs. r = 0.70). At some locations, the RAP-Chem performed poorly for tree and grass pollen (e.g., Springfield, MO), though the time series at this site is very short, and the model demonstrated high skill at other sites (e.g., r = 0.73 for tree pollen at Raleigh, NC, r = 0.81 for grass pollen at Waco, TX). The superior performance for RAP-Chem weed pollen (r(Pollen Sense) = 0.58–0.85) is likely twofold: first, the weed category in PECM is represented by a single genus that is the dominant weed over North America (*Ambrosia*), eliminating errors introduced by lumping multiple genera with varying phenology (i.e., as with tree pollen); second, the distinct morphology of ragweed pollen may be more consistently identified by the Pollen Sense identification algorithm. To be sure, Pollen Sense includes weed genera other than ragweed, which may explain the spring weed signal and its earlier SOS compared to RAP-Chem. Phenological timing is similar between RAP-Chem and Pollen Sense across the NAB sites; mean absolute error (MAE) for tree, grass, and weed pollen of 21.0/13.9/22.4 d, 5.2/18.4/6.6 d, and 19.2/44.2/21.4 d, respectively for Pollen Sense; MAE = 19.9/20.7/13.8 d, 24.0/17.6/12.2 d, and 32.8/65.2/12.2 d for RAP-Chem. US-wide, RAP-Chem and Pollen Sense phenology agree best for weed pollen and poorest for tree pollen SOS and grass pollen EOS.

Across North America, RAP-Chem overestimated tree pollen in heavily forested regions (i.e., the eastern US, Pacific Northwest, and Canada) and underestimated tree pollen in the lower Mississippi River Valley. Grass and weed pollen were generally underestimated (Fig. 3i–l), though these biases should be interpreted with caution, as the post hoc gravitational settling correction (α = 0.0136; Sect. 2.4) reduces concentrations by ~74x and depends on the definition of an a priori surface removal velocity. Tree pollen is not settling-corrected (α = 1), and its high biases over extensive forests likely reflect both PECM emission uncertainties and the omitted settling (Sect. 2.4), though few Pollen Sense monitors exist in many of these locations.

Several systematic biases and limitations remain within the modeling framework, highlighting multiple fundamental uncertainties inherent in current pollen modeling:

https://doi.org/10.5194/egusphere-2026-6663
Preprint. Discussion started: 16 November 2026
© Author(s) 2026. CC BY 4.0 License.

- Representing all tree and grass pollen with a single 20 μm grain diameter introduces error in the size-dependent removal parametrizations (e.g., pine pollen (~70 μm) settling would be ~12x faster). Even if it had included gravitational settling, RAP-Chem would have underestimated pine pollen settling (and misrepresented its radiation impacts, though not explored here). Converting model output back to grains with the lumped diameter neglects the inter-genera variation in size in the original emissions. Future work will explore representing pollen using a size-resolved or number concentration-aware approach (i.e., a two-moment scheme) to allow for more physically consistent representations of pollen without adding significant computational burden (e.g., requiring each genus is represented as a separate tracer, though this may be useful for targeted allergenic-focused simulations).
- Neglecting gravitational settling for coarse pollen clearly introduced a significant error in RAP-Chem's pollen magnitudes. We corrected grass and weed pollen post hoc due to emission vs. measurement height mismatches. Future versions of the model will include this process.
- Some tree pollen should likely be emitted above the lowest model layer, particularly when the lowest model layer is relatively thin (here, 16 m). Further, future model–observation comparisons should include both the first and second layer of the model to understand the sensitivity to these parameterizations.
- Evaluating forecast skill using only total pollen can substantially misrepresent it. Total pollen correlations (r = 0.44 vs. NAB) were lower than the correlations for grass (0.53) and weed (0.74), likely because errors in the dominant pollen class (i.e., trees) propagate into the total. Accordingly, pollen forecasts should be verified against individual classes whenever possible.
- The parameterization of pollen rupture due to high relative humidity or lightning, which converts 10% (lightning) to 70% (relative humidity) of intact pollen into SPPs, is physically necessary to capture real-world pollen dynamics and cloud–aerosol interactions, but the process remains highly unconstrained. Over- or under-predicting rupture rates directly impacts the simulated concentration of intact grains at the surface. However, returning all SPP mass to intact pollen only marginally changed the correlations (≤ 0.02; Table 2 vs. Table S6). Constraining the rupture mechanism will likely require laboratory evaluations of the process and/or careful evaluation of health impacts.
- Areas with the lowest model–observation correlations (such as the Intermountain West, and parts of Canada) coincide with the largest gaps in the Pollen Sense network. Consequently, poor statistical agreement in these regions may be an artifact of spatial interpolation or model error. In any case, there is a large need to expand the capabilities of current pollen monitoring systems, especially in less-populated areas.

Despite these challenges, the implementation of a prognostic pollen framework within a real-time forecast like RAP-Chem, though experimental, represents a vital step forward for both numerical weather prediction and public health. By explicitly simulating the emission, transport, and rupture of pollen into SPPs, we lay the groundwork for better forecasting of severe respiratory events, such as "thunderstorm asthma", while potentially improving the physical accuracy of the underlying meteorological model. Because we did not perform a baseline meteorological sensitivity simulation without pollen, quantifying

https://doi.org/10.5194/egusphere-2026-6663
Preprint. Discussion started: 16 November 2026
© Author(s) 2026. CC BY 4.0 License.

the precise impact of pollen on the RAP-Chem weather forecast is beyond the scope of this evaluation and is reserved for future work. To be sure, other groups are actively researching this topic (Matthews et al., 2023; Zhang et al., 2024).

The value of a pollen forecast is largely in its ability to predict the phenological timing, daily variations, and relative magnitudes of pollen classes rather than absolute concentrations (e.g., low/moderate/high/very high). Our results indicate that RAP-Chem has more skill in reproducing season timing and multi-day episodes (i.e., correlations improve with five-day smoothing) as compared to absolute magnitudes (though there are many uncertainties). However, systematic biases are a fundamental issue across numerical weather prediction and air quality forecasts. Operational air quality forecasts are frequently bias-corrected in real time (Djalalova et al., 2015; Huang et al., 2017; Kang et al., 2010). Operational pollen forecasts also use these approaches; e.g., the European ensemble of the Copernicus Atmosphere Monitoring Service (ECMWF CAMS) is still used for advisories because of the skill in reproducing pollen timing (Colette et al., 2025; Prank et al., 2013; Sofiev et al., 2015, 2017). The gravitational settling correction applied here (Sect. 2.4) is analogous to these bias corrections. Importantly, because it is a single scaling factor, it affects only the magnitude of the forecast and leaves *r* and phenological timing (SOS, POS, and EOS) unchanged.

Future work should focus on refining emission potentials using higher-resolution, species-specific land use datasets in synergy with land surface model development and improving the parameterization of humidity- and lightning-induced pollen rupture. Season timing is another area for potential improvement. PECM determines pollen season phenology at the beginning of the forecast year from the previous year's annual mean temperature, so simulated phenology cannot respond to current year seasonality anomalies. The near-real-time availability of Pollen Sense introduces the potential for data assimilation of observations at the time of the forecast to correct emissions, rather than using the emissions built solely on climatological relationships.

The public health utility of a coupled emission-transport model is clear. Transitioning from delayed, point-based daily observations to a continuous gridded forecast provides a crucial tool for exposure management. For the millions of Americans suffering from pollen allergies, high-resolution forecasts allow for locally informed management of outdoor activities and medication. Furthermore, by explicitly simulating both the transport and the rupture of intact grains into SPPs, forecasting systems like RAP-Chem lay the critical groundwork for early warning systems targeting severe, acute respiratory events such as thunderstorm asthma, ultimately reducing the burden on healthcare systems and mitigating lost economic productivity.

https://doi.org/10.5194/egusphere-2026-6663
Preprint. Discussion started: 16 November 2026
© Author(s) 2026. CC BY 4.0 License.

Code and data availability

The RAP-Chem model code, daily RAP-Chem output, PECM pollen emission potentials, and NAB data are currently under review at Zenodo as a draft. The final DOI will be 10.5281/zenodo.23696901 (Schnell, 2026) and the reviewers can privately access the files with a temporary link:
https://zenodo.org/records/23696901?preview=1&token=eyJhbGciOiJIUzUxMiJ9.eyJpZCI6IjVmYWU4NWQwLWQ1NmEtNDhhMS1iNjExLWM1ZDdlZmRhNzY0ZSIsImRhdGEiOnt9LCJyYW5kb20iOiJiYWZjZDY0NDUwZDc1ZDlhMGMyYzM0NTNiNjQyMjZhZiJ9.cQDvEfKJ-R6SFl5Gb5ybPvFyUp84dq9332YEg9-U7m7Rih6H8nifM4odrMIA2W9CIQ0Txm5Qx5zd4kue0I_Igg. Pollen Sense data may be made available from the corresponding author upon reasonable request due to licensing restrictions.

Supplement link

The link to the supplement will be included by Copernicus, if applicable.

Author contributions

JS, AS, RA, YZ, and TS contributed to the RAP-Chem and/or PECM model code. JS carried out the experimental forecasts, performed the data analysis, and led the writing of the paper. AC, NA, and SK provided supplemental figures and tables and led the collection of the Pollen Sense measurements. DF and GR collected NAB observations. All authors provided input to the paper.

Competing interests

The authors declare that they have no conflict of interest.

Disclaimer

The statements, findings, conclusions, and recommendations are those of the author(s) and do not necessarily reflect the views of NOAA or the U.S. Department of Commerce.

Acknowledgements

The authors wish to thank the administrators of the Jet supercomputer in Boulder, CO for their tireless efforts maintaining the computing environment and system. We thank Dr. Bill Palmer and the Boise Valley Asthma & Allergy Clinic for allowing the use of their historical pollen counts. We also thank Mariel Delgado Cruz, Shane Brinker, Cathy Johnson,

https://doi.org/10.5194/egusphere-2026-6663
Preprint. Discussion started: 16 November 2026
© Author(s) 2026. CC BY 4.0 License.

Jeremy Quinton and Katie Brite for collecting and sharing the data from the Springfield-Greene County Health Department. We also thank Christina Utz at the Houston Health Department for sharing their historical pollen counts. We also thank the North Carolina Division of Air Quality's Pollen Laboratory for providing their historical pollen counts. We also thank Wayne Wilhelm at the St. Louis County Department of Public Health for providing their historical pollen counts. We also thank Cheryl Jenkins and the Allergy and Asthma Care of Waco for their pollen measurements. We also thank Atlanta Allergy & Asthma for their pollen measurements. We acknowledge the use of Google Gemini (Pro) and Claude (Opus 4.8 and 5.5) to assist in the data analysis and plot generation scripts.

Financial support

This research was supported in part by the NOAA cooperative agreement NA22OAR4320151, for the Cooperative Institute for Earth System Research and Data Science (CIESRDS). We also thank the NOAA Climate Program Office (CPO) for supporting this work through the Earth Radiation Budget (ERB) and Atmospheric Chemistry, Carbon Cycle, and Climate (AC4) programs.

References

Ahmadov, R., McKeen, S. A., Robinson, A. L., Bahreini, R., Middlebrook, A. M., De Gouw, J. A., Meagher, J., Hsie, E. -Y., Edgerton, E., Shaw, S., and Trainer, M.: A volatility basis set model for summertime secondary organic aerosols over the eastern United States in 2006, J. Geophys. Res. Atmos., 117, 2011JD016831, https://doi.org/10.1029/2011JD016831, 2012.

Benjamin, S. G., Weygandt, S. S., Brown, J. M., Hu, M., Alexander, C. R., Smirnova, T. G., Olson, J. B., James, E. P., Dowell, D. C., Grell, G. A., Lin, H., Peckham, S. E., Smith, T. L., Moninger, W. R., Kenyon, J. S., and Manikin, G. S.: A North American Hourly Assimilation and Model Forecast Cycle: The Rapid Refresh, Mon. Weather Rev., 144, 1669–1694, https://doi.org/10.1175/MWR-D-15-0242.1, 2016.

Buters, J., Clot, B., Galán, C., Gehrig, R., Gilge, S., Hentges, F., O'Connor, D., Sikoparija, B., Skjoth, C., Tummon, F., Adams-Groom, B., Antunes, C. M., Bruffaerts, N., Çelenk, S., Crouzy, B., Guillaud, G., Hajkova, L., Seliger, A. K., Oliver, G., Ribeiro, H., Rodinkova, V., Saarto, A., Sauliene, I., Sozinova, O., and Stjepanovic, B.: Automatic detection of airborne pollen: an overview, Aerobiologia, 40, 13–37, https://doi.org/10.1007/s10453-022-09750-x, 2024.

Clough, S. A., Shephard, M. W., Mlawer, E. J., Delamere, J. S., Iacono, M. J., Cady-Pereira, K., Boukabara, S., and Brown, P. D.: Atmospheric radiative transfer modeling: a summary of the AER codes, J. Quant. Spectrosc. Radiat. Transf., 91, 233–244, https://doi.org/10.1016/j.jqsrt.2004.05.058, 2005.

Colette, A., Collin, G., Besson, F., Blot, E., Guidard, V., Meleux, F., Royer, A., Petiot, V., Miller, C., Fermond, O., Jeant, A., Adani, M., Arteta, J., Benedictow, A., Bergström, R., Bowdalo, D., Brandt, J., Briganti, G., Carvalho, A. C., Christensen, J. H., Couvidat, F., D'Elia, I., D'Isidoro, M., Denier van der Gon, H., Descombes, G., Di Tomaso, E., Douros, J., Escribano,

https://doi.org/10.5194/egusphere-2026-6663
Preprint. Discussion started: 16 November 2026
© Author(s) 2026. CC BY 4.0 License.

J., Eskes, H., Fagerli, H., Fatahi, Y., Flemming, J., Friese, E., Frohn, L., Gauss, M., Geels, C., Guarnieri, G., Guevara, M., Guion, A., Guth, J., Hänninen, R., Hansen, K., Im, U., Janssen, R., Jeoffrion, M., Joly, M., Jones, L., Jorba, O., Kadantsev, E., Kahnert, M., Kaminski, J. W., Kouznetsov, R., Kranenburg, R., Kuenen, J., Lange, A. C., Langner, J., Lannuque, V., Macchia, F., Manders, A., Mircea, M., Nyiri, A., Olid, M., Pérez García-Pando, C., Palamarchuk, Y., Piersanti, A., Raux, B., Razinger, M., Robertson, L., Segers, A., Schaap, M., Siljamo, P., Simpson, D., Sofiev, M., Stangel, A., Struzewska, J., Tena, C., Timmermans, R., Tsikerdekis, T., Tsyro, S., Tyuryakov, S., Ung, A., Uppstu, A., Valdebenito, A., van Velthoven, P., Vitali, L., Ye, Z., Peuch, V.-H., and Rouïl, L.: Copernicus Atmosphere Monitoring Service – Regional Air Quality Production System v1.0, Geosci. Model Dev., 18, 6835–6883, https://doi.org/10.5194/gmd-18-6835-2025, 2025.

Coye, P., Willitsford, A. H., and Winstead, N.: Operational Performance of High-Resolution Rapid Refresh (HRRR) Smoke Forecasting during the Canadian Wildfires of Summer 2023, Weather Forecast., 41, 1289–1300, https://doi.org/10.1175/WAF-D-25-0211.1, 2026.

Crystal-Peters, J., Crown, W. H., Goetzel, R. Z., and Schutt, D. C.: The cost of productivity losses associated with allergic rhinitis, Am. J. Manag. Care, 6, 373–378, 2000.

Damialis, A., Kaimakamis, E., Konoglou, M., Akritidis, I., Traidl-Hoffmann, C., and Gioulekas, D.: Estimating the abundance of airborne pollen and fungal spores at variable elevations using an aircraft: how high can they fly?, Sci. Rep., 7, 44535, https://doi.org/10.1038/srep44535, 2017.

Djalalova, I., Delle Monache, L., and Wilczak, J.: PM2.5 analog forecast and Kalman filter post-processing for the Community Multiscale Air Quality (CMAQ) model, Atmos. Environ., 108, 76–87, https://doi.org/10.1016/j.atmosenv.2015.02.021, 2015.

Farooq, Q., Oteros, J., and Galán, C.: Advancing in the pollen frontier: a comprehensive evaluation and meta-analysis of automatic pollen monitoring systems, Aerobiologia, 41, 527–546, https://doi.org/10.1007/s10453-025-09865-x, 2025.

Freitas, S. R., Grell, G. A., and Li, H.: The Grell–Freitas (GF) convection parameterization: recent developments, extensions, and applications, Geosci. Model Dev., 14, 5393–5411, https://doi.org/10.5194/gmd-14-5393-2021, 2021.

Grell, G. A., Peckham, S. E., Schmitz, R., McKeen, S. A., Frost, G., Skamarock, W. C., and Eder, B.: Fully coupled "online" chemistry within the WRF model, Atmos. Environ., 39, 6957–6975, https://doi.org/10.1016/j.atmosenv.2005.04.027, 2005.

Huang, J., McQueen, J., Wilczak, J., Djalalova, I., Stajner, I., Shafran, P., Allured, D., Lee, P., Pan, L., Tong, D., Huang, H.-C., DiMego, G., Upadhayay, S., and Delle Monache, L.: Improving NOAA NAQFC PM2.5 Predictions with a Bias Correction Approach, Weather Forecast., 32, 407–421, https://doi.org/10.1175/WAF-D-16-0118.1, 2017.

James, E. P., Alexander, C. R., Dowell, D. C., Weygandt, S. S., Benjamin, S. G., Manikin, G. S., Brown, J. M., Olson, J. B., Hu, M., Smirnova, T. G., Ladwig, T., Kenyon, J. S., and Turner, D. D.: The High-Resolution Rapid Refresh (HRRR): An Hourly Updating Convection-Allowing Forecast Model. Part II: Forecast Performance, Weather Forecast., 37, 1397–1417, https://doi.org/10.1175/WAF-D-21-0130.1, 2022.

Jiang, C., Wang, W., Du, L., Huang, G., McConaghy, C., Fineman, S., and Liu, Y.: Field Evaluation of an Automated Pollen Sensor, Int. J. Environ. Res. Public. Health, 19, 6444, https://doi.org/10.3390/ijerph19116444, 2022.

https://doi.org/10.5194/egusphere-2026-6663
Preprint. Discussion started: 16 November 2026
© Author(s) 2026. CC BY 4.0 License.

Kang, D., Mathur, R., and Trivikrama Rao, S.: Real-time bias-adjusted O3 and PM2.5 air quality index forecasts and their performance evaluations over the continental United States, Atmos. Environ., 44, 2203–2212, https://doi.org/10.1016/j.atmosenv.2010.03.017, 2010.

Li, Y., Pickering, K. E., Barth, M. C., Bela, M. M., Cummings, K. A., and Allen, D. J.: Evaluation of Parameterized Convective Transport of Trace Gases in Simulation of Storms Observed During the DC3 Field Campaign, J. Geophys. Res. Atmos., 123, https://doi.org/10.1029/2018JD028779, 2018.

Lucas, R. W. and Bunderson, L.: A Review of Pollen Counting Networks: From the Nineteenth Century into the Twenty-first Century, Curr. Allergy Asthma Rep., 24, 1–9, https://doi.org/10.1007/s11882-023-01119-5, 2024.

Matthews, B. H., Alsante, A. N., and Brooks, S. D.: Pollen Emissions of Subpollen Particles and Ice Nucleating Particles, ACS Earth Space Chem., 7, 1207–1218, https://doi.org/10.1021/acsearthspacechem.3c00014, 2023.

Maya-Manzano, J. M., Tummon, F., Abt, R., Allan, N., Bunderson, L., Clot, B., Crouzy, B., Daunys, G., Erb, S., Gonzalez-Alonso, M., Graf, E., Grewling, Ł., Haus, J., Kadantsev, E., Kawashima, S., Martinez-Bracero, M., Matavulj, P., Mills, S., Niederberger, E., Lieberherr, G., Lucas, R. W., O'Connor, D. J., Oteros, J., Palamarchuk, J., Pope, F. D., Rojo, J., Šaulienė, I., Schäfer, S., Schmidt-Weber, C. B., Schnitzler, M., Šikoparija, B., Skjøth, C. A., Sofiev, M., Stemmler, T., Triviño, M., Zeder, Y., and Buters, J.: Towards European automatic bioaerosol monitoring: Comparison of 9 automatic pollen observational instruments with classic Hirst-type traps, Sci. Total Environ., 866, 161220, https://doi.org/10.1016/j.scitotenv.2022.161220, 2023.

Meltzer, E. O. and Bukstein, D. A.: The economic impact of allergic rhinitis and current guidelines for treatment, Ann. Allergy Asthma Immunol. Off. Publ. Am. Coll. Allergy Asthma Immunol., 106, S12-16, https://doi.org/10.1016/j.anai.2010.10.014, 2011.

Ng, A. and Boersma, P.: Diagnosed Allergic Conditions in Adults: United States, 2021, National Center for Health Statistics (U.S.), https://doi.org/10.15620/cdc:122809, 2023.

Olson, J., Angevine, W. M., Turner, D. D., Sun, X., Simonson, J. M., Evans, C., Kenyon, J. S., Li, H., Schnell, J., Puhales, F. S., Cherubini, T., Li, W., and Zhang, M.: A Description of the MYNN-EDMF Turbulence Scheme, NOAA Tech. Memo. OAR GSL 77, https://doi.org/10.25923/RAHR-SJ70, 2026.

Posselt, R. and Lohmann, U.: Influence of Giant CCN on warm rain processes in the ECHAM5 GCM, Atmos. Chem. Phys., 8, 3769–3788, https://doi.org/10.5194/acp-8-3769-2008, 2008.

Prank, M., Chapman, D. S., Bullock, J. M., Belmonte, J., Berger, U., Dahl, A., Jäger, S., Kovtunenko, I., Magyar, D., Niemelä, S., Rantio-Lehtimäki, A., Rodinkova, V., Sauliene, I., Severova, E., Sikoparija, B., and Sofiev, M.: An operational model for forecasting ragweed pollen release and dispersion in Europe, Agric. For. Meteorol., 182–183, 43–53, https://doi.org/10.1016/j.agrformet.2013.08.003, 2013.

Rojo, J., Oteros, J., Pérez-Badia, R., Cervigón, P., Ferencova, Z., Gutiérrez-Bustillo, A. M., Bergmann, K.-C., Oliver, G., Thibaudon, M., Albertini, R., Rodríguez-De La Cruz, D., Sánchez-Reyes, E., Sánchez-Sánchez, J., Pessi, A.-M., Reiniharju, J., Saarto, A., Calderón, M. C., Guerrero, C., Berra, D., Bonini, M., Chiodini, E., Fernández-González, D., García, J., Trigo,

https://doi.org/10.5194/egusphere-2026-6663
Preprint. Discussion started: 16 November 2026
© Author(s) 2026. CC BY 4.0 License.

M. M., Myszkowska, D., Fernández-Rodríguez, S., Tormo-Molina, R., Damialis, A., Kolek, F., Traidl-Hoffmann, C., Severova, E., Caeiro, E., Ribeiro, H., Magyar, D., Makra, L., Udvardy, O., Alcázar, P., Galán, C., Borycka, K., Kasprzyk, I., Newbigin, E., Adams-Groom, B., Apangu, G. P., Frisk, C. A., Skjøth, C. A., Radišić, P., Šikoparija, B., Celenk, S., Schmidt-Weber, C. B., and Buters, J.: Near-ground effect of height on pollen exposure, Environ. Res., 174, 160–169, https://doi.org/10.1016/j.envres.2019.04.027, 2019.

Scheifinger, H., Belmonte, J., Buters, J., Celenk, S., Damialis, A., Dechamp, C., García-Mozo, H., Gehrig, R., Grewling, L., Halley, J. M., Hogda, K.-A., Jäger, S., Karatzas, K., Karlsen, S.-R., Koch, E., Pauling, A., Peel, R., Sikoparija, B., Smith, M., Galán-Soldevilla, C., Thibaudon, M., Vokou, D., and De Weger, L. A.: Monitoring, Modelling and Forecasting of the Pollen Season, in: Allergenic Pollen, edited by: Sofiev, M. and Bergmann, K.-C., Springer Netherlands, Dordrecht, 71–126, https://doi.org/10.1007/978-94-007-4881-1_4, 2013.

Schnell, J., 2026. Supporting data for Schnell et al., "NOAA Global Systems Laboratory experimental pollen forecasting using the Pollen Emissions for Climate Models (PECM) with the Rapid-Refresh coupled to Chemistry (RAP-Chem) model", https://doi.org/10.5281/zenodo.23696901.

Schnell, J., Ahmadov, R., Grell, G. A., Olson, J. B., James, E., Hu, M., Wong, K. Y., McDonald, B., Schwantes, R. H., He, J., Harkins, C., Angevine, W. M., Jamison, B., Pierce, R. B., Coggon, M., Baker, B., Freitas, S., Pereira, G., and Tsidulko, M.: Tight physics and chemistry coupling improves air quality forecasts: a case study of the 2020 North American wildfires with the Rapid Refresh model coupled to Chemistry (RAP-Chem v1.0), https://doi.org/10.5194/egusphere-2026-4786, 13 August 2026., 2026.

Seinfeld, J. H. and Pandis, S. N.: Atmospheric chemistry and physics: from air pollution to climate change, Third edition., John Wiley & Sons, Inc, Hoboken, New Jersey, 1120 pp., 2016.

Shah, D., Ford, L., Ochkur, S., Kosisky, S., Fineman, S., Virant, F., and Rank, M.: Accuracy of spring pollen forecasts in five U.S. cities using National Allergy Bureau reporting as a gold standard, J. Allergy Clin. Immunol. Pract., 12, 1633–1635, https://doi.org/10.1016/j.jaip.2024.02.020, 2024.

Smirnova, T. G., Brown, J. M., Benjamin, S. G., and Kenyon, J. S.: Modifications to the Rapid Update Cycle Land Surface Model (RUC LSM) Available in the Weather Research and Forecasting (WRF) Model, Mon. Weather Rev., 144, 1851–1865, https://doi.org/10.1175/MWR-D-15-0198.1, 2016.

Sofiev, M., Berger, U., Prank, M., Vira, J., Arteta, J., Belmonte, J., Bergmann, K.-C., Chéroux, F., Elbern, H., Friese, E., Galan, C., Gehrig, R., Khvorostyanov, D., Kranenburg, R., Kumar, U., Marécal, V., Meleux, F., Menut, L., Pessi, A.-M., Robertson, L., Ritenberga, O., Rodinkova, V., Saarto, A., Segers, A., Severova, E., Sauliene, I., Siljamo, P., Steensen, B. M., Teinemaa, E., Thibaudon, M., and Peuch, V.-H.: MACC regional multi-model ensemble simulations of birch pollen dispersion in Europe, Atmos. Chem. Phys., 15, 8115–8130, https://doi.org/10.5194/acp-15-8115-2015, 2015.

Sofiev, M., Ritenberga, O., Albertini, R., Arteta, J., Belmonte, J., Bernstein, C. G., Bonini, M., Celenk, S., Damialis, A., Douros, J., Elbern, H., Friese, E., Galan, C., Oliver, G., Hrga, I., Kouznetsov, R., Krajsek, K., Magyar, D., Parmentier, J., Plu, M., Prank, M., Robertson, L., Steensen, B. M., Thibaudon, M., Segers, A., Stepanovich, B., Valdebenito, A. M., Vira, J.,

https://doi.org/10.5194/egusphere-2026-6663
Preprint. Discussion started: 16 November 2026
© Author(s) 2026. CC BY 4.0 License.

and Vokou, D.: Multi-model ensemble simulations of olive pollen distribution in Europe in 2014: current status and outlook, Atmos. Chem. Phys., 17, 12341–12360, https://doi.org/10.5194/acp-17-12341-2017, 2017.

Steiner, A. L., Brooks, S. D., Deng, C., Thornton, D. C. O., Pendleton, M. W., and Bryant, V.: Pollen as atmospheric cloud condensation nuclei, Geophys. Res. Lett., 42, 3596–3602, https://doi.org/10.1002/2015GL064060, 2015.

Subba, T., Zhang, Y., and Steiner, A. L.: Simulating the Transport and Rupture of Pollen in the Atmosphere, J. Adv. Model. Earth Syst., 15, e2022MS003329, https://doi.org/10.1029/2022MS003329, 2023.

Tang, M., Gu, W., Ma, Q., Li, Y. J., Zhong, C., Li, S., Yin, X., Huang, R.-J., He, H., and Wang, X.: Water adsorption and hygroscopic growth of six anemophilous pollen species: the effect of temperature, Atmos. Chem. Phys., 19, 2247–2258, https://doi.org/10.5194/acp-19-2247-2019, 2019.

Thompson, G. and Eidhammer, T.: A Study of Aerosol Impacts on Clouds and Precipitation Development in a Large Winter Cyclone, J. Atmos. Sci., 71, 3636–3658, https://doi.org/10.1175/JAS-D-13-0305.1, 2014.

Wozniak, M. C. and Steiner, A. L.: A prognostic pollen emissions model for climate models (PECM1.0), Geosci. Model Dev., 10, 4105–4127, https://doi.org/10.5194/gmd-10-4105-2017, 2017.

Yin, Y., Levin, Z., Reisin, T. G., and Tzivion, S.: The effects of giant cloud condensation nuclei on the development of precipitation in convective clouds — a numerical study, Atmos. Res., 53, 91–116, https://doi.org/10.1016/S0169-8095(99)00046-0, 2000.

Zhang, L.: A size-segregated particle dry deposition scheme for an atmospheric aerosol module, Atmos. Environ., 35, 549–560, https://doi.org/10.1016/S1352-2310(00)00326-5, 2001.

Zhang, L., Montuoro, R., McKeen, S. A., Baker, B., Bhattacharjee, P. S., Grell, G. A., Henderson, J., Pan, L., Frost, G. J., McQueen, J., Saylor, R., Li, H., Ahmadov, R., Wang, J., Stajner, I., Kondragunta, S., Zhang, X., and Li, F.: Development and evaluation of the Aerosol Forecast Member in the National Center for Environment Prediction (NCEP)'s Global Ensemble Forecast System (GEFS-Aerosols v1), Geosci. Model Dev., 15, 5337–5369, https://doi.org/10.5194/gmd-15-5337-2022, 2022.

Zhang, X., Wang, W., Saburi, Y., Paduch, H. R., Jin, Z., Zhu, K., and Liu, Y.: Estimating Daily Taxon-specific Tree Pollen at a 1-km Resolution in Atlanta, GA from 2020 to 2024, bioRxiv, 2026.05.14.725192, https://doi.org/10.64898/2026.05.14.725192, 2026.

Zhang, Y. and Steiner, A. L.: Projected climate-driven changes in pollen emission season length and magnitude over the continental United States, Nat. Commun., 13, 1234, https://doi.org/10.1038/s41467-022-28764-0, 2022.

Zhang, Y., Subba, T., Matthews, B. H., Pettersen, C., Brooks, S. D., and Steiner, A. L.: Effects of Pollen on Hydrometeors and Precipitation in a Convective System, J. Geophys. Res. Atmos., 129, e2023JD039891, https://doi.org/10.1029/2023JD039891, 2024.

Zhu, X., Ma, X., Zhang, Z., Liu, Y., Luo, Y., Yan, K., Pei, T., and Huete, A.: Floating in the air: forecasting allergenic pollen concentration for managing urban public health, Int. J. Digit. Earth, 17, 2306894, https://doi.org/10.1080/17538947.2024.2306894, 2024.